NUMERICAL MODELING OF DYNAMICS OF SANDWICH PLATES WITH PARTIALLY DAMAGED FACESHEET-TO-CORE INTERFACE

[1,2]Burlayenko V. N., [1]Sadowski T., [2]Nazarenko S.A.

[1] Lublin University of Technology, Lublin, Poland
[2] National Technical University 'KhPI', Kharkov, Ukraine

The complex inherent structure of sandwich materials, including highly dissimilar constitutive layers leads to appearance of a new type of damage modes, where a partial separation between basic layers, the facesheet and core, of the sandwich panel so-called debonding is one of the most common defects among them. In the case of dynamic loading, this effect manifests itself by the alternation of natural frequencies, damping ratios and time-history responses. Therefore, in order to guarantee the safe performance of sandwich structural components, a good understanding of their vibration behavior has to be provided. On the other hand, the vibration characteristics of damaged structures can be useful for an on-line detection of defects (non-destructive testing) without actually dismantling the structures. Thus the vibration analysis of sandwich panels can be considered in the frameworks of damage detection problems as well.

Vibration problems of composite structures such as sandwich and laminated panels with an imperfect interface between basic layers have attracted an intensive research interest. In order to tackle this complicated problem different approaches have been proposed. The earliest analytical model of composite beams with a local interface defect (delamination) was proposed in [1]. The 'free mode model', developed using the split span wise approach, neglected contact between freely vibrated detached surfaces. The model was used to solve an egienvalue problem. Wang et al. [2] improved this model by including the coupling between flexural and longitudinal motion in the free vibration analysis. Authors in [3] suggested a new, so-called 'constrained mode model' relaying on the assumption that the detached surfaces identically move in the transverse direction for freely vibrated composite beam. To simulate the interaction between upper and lower crack surfaces, a piecewise linear spring model was applied in [4] for obtaining an eigensolution. A nonlinear spring model for describing the impenetrability behavior of detached parts was proposed in [5] to model free and forced oscillations of a composite beam.

In the case when the dimension of the problem under consideration is more than one, the use of numerical methods based mainly on the finite element method (FEM) is needed. Two-dimensional models applied to the free vibration analysis of cracked laminated beams and plates can be found, e.g. in [6]. The extended FEM adopted to analyze free vibrations of 2-D cracked plates was used in [7]. A FE model of laminated plates based on the three-dimensional theory was developed in [8] and a mixed model with shell finite elements for facesheets and 3-D elements for the core was presented in [8]. A comprehensive summary

on modeling techniques used to perform the free vibration analysis of debonded and delaminated (in the case of laminated structures) composite beams, plates and shells is done by Della and Shu [9]. The use of vibration characteristics for vibration-based damage detection methods has been recently reviewed in [10].

If one considers the repetitive opening and closing of the separated surfaces, a case that is referred to as a closing or breathing crack, then the system is highly nonlinear. One of approaches commonly used in vibration theory of cracked structures is the replacing of the continuous cracked structure with a single-DOF or multi-DOF oscillator model, e.g. [12,13]. Those models were successful to reveal nonlinear response of studied systems such as super- and subharmonics resonances and period doubling bifurcations. Recent investigations on the dissipative character of impact-like contacts in delaminated beams with an oscillator model within non-smooth mechanics can be found in [14].

While the oscillator models, used in those studies allowed bringing the light on nonlinear phenomena of cracked structures they suffer from the lack to give a spatial presentation of a continuous structure. This issue is being easily overcome by numerical modeling techniques. For instance, the 2-D elastodynamic problem of a plate with one and two co-linear cracks of finite length subjected to tension-compression harmonic loading with unilateral contact interaction at the crack edges was solved by boundary element method in [15]. Ju et al. [16] have studied forced vibrations of delaminated beams with intermittent contact in delaminated segments by employing the FEM. The perturbation method within the concept of nonlinear normal modes was applied in [17] to study vibrations of delaminated beams. The Galerkin method and harmonic balance method were employed in [18] to find solutions of beam-plates with a delamination undergoing nonlinear free vibration. Contact-impact conditions to the separated faces of a debonded sandwich beam discretized by plate finite elements were applied via appropriate contact elements in [19]. To prevent penetration at delamination interfaces, unilateral contact constraints by Lagrange multiplier method were imposed in the FE time response analysis of a composite plate with multiple delaminations in [20]. A semi-analytical approach for studying free oscillations and transient dynamics of simply supported debonded sandwich beams accounting for a contact interaction between the detached parts was proposed in [21]. A further contribution into a nonlinear dynamic behavior of sandwich plates with an imperfect interface can be found in [22], where the case of a sandwich plate containing a post-impact zone was considered by a 3-D FE model in the ABAQUS code.

The aim of this paper is to investigate a dynamic behavior of sandwich plates with debonding by numerical simulations. A computational model of sandwich plate in FE software is developed involving features of the contact problem between debonded parts and finite-element procedure with explicit time integration. The forced vibration analysis is discussed.

1. Governing Equations. In this section the mathematical aspects of the general elastodynamic problem of a body with intermittent interactions at separated

interfaces are briefly discussed. For further details, we refer to [23]. Here, we will use notations that are usual in continuum mechanics.
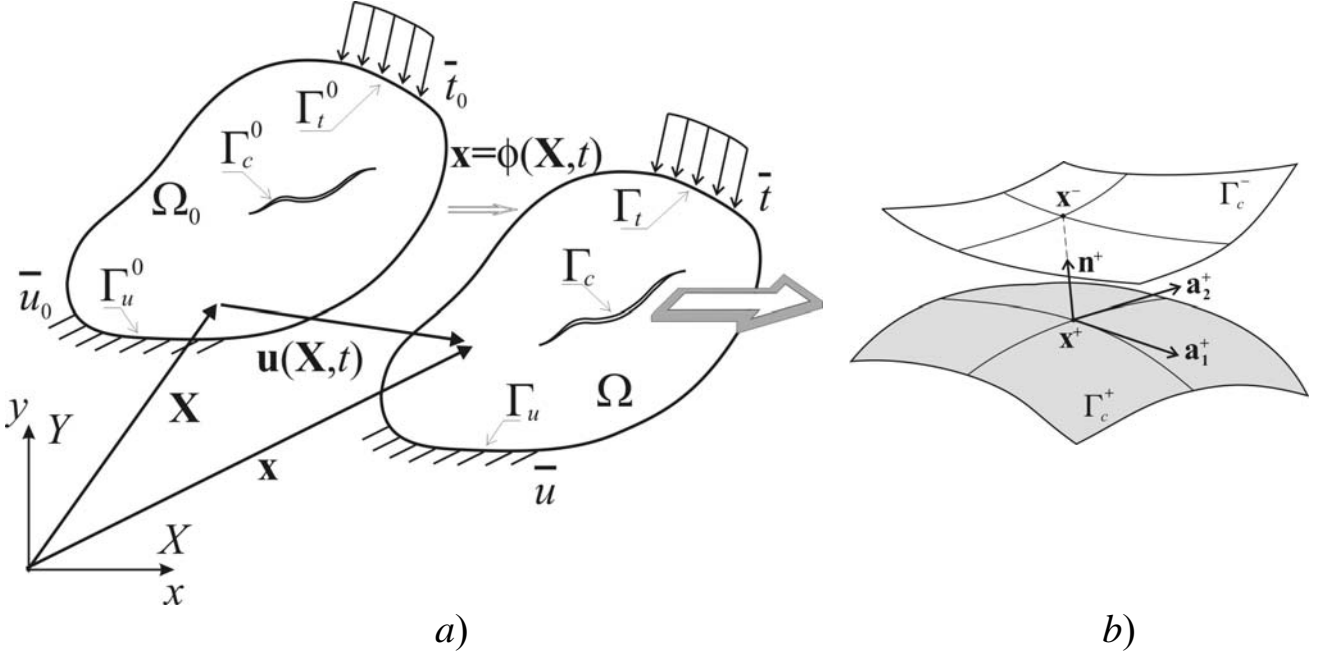

a)   *b)*

Fig.1. A body with a discontinuity and its representation in the reference and the current domains (*a*) and zoom of the discontinuity surfaces (*b*).

Let us consider an initial (reference) domain $\Omega_0 \in \Re^3$ and its boundary Γ^0 as shown in Fig. 1*a*. In doing so, $\Gamma_t^0 \cup \Gamma_u^0 = \Gamma^0$ and $\Gamma_t^0 \cap \Gamma_u^0 = \varnothing$, where Γ_t^0 and Γ_u^0 are parts of the boundary with prescribed tractions and displacements, respectively. We allow this domain to contain an internal discontinuity, e.g. described by Γ_c^0. Let $\widetilde{\Omega}_0$ be the open set, which excludes all discontinuities, i.e. $\widetilde{\Omega}_0 = \Omega_0 \setminus \Gamma_c^0$. In the current (deformed) domain, the images of the initial domain Ω_0 and $\widetilde{\Omega}_0$ are denoted by Ω and $\widetilde{\Omega}$, respectively as well as for all other notations, and the motion is described by $\mathbf{x} = \varphi(\mathbf{X}, t)$, where $t \in [0, T]$ is the time, and $\mathbf{X}$ and $\mathbf{x}$ are material and spatial co-ordinates, respectively. In the motion, the displacement at the material point $\mathbf{X}$ is denoted by $\mathbf{u}(\mathbf{X}, t)$. We assume that strains and rotations of the body are small and the elastic behavior of the body is characterized by the Cauchy law. Thus, the linear body considered in the Lagrangian description will be governed by the equations presented below.

The linear momentum equation is given by

$$\frac{\partial \sigma_{ji}}{\partial x_j} + \rho b_i = \rho \ddot{u}_i \text{ in } \widetilde{\Omega} \times [0, T], \tag{1}$$

where ρ is the current mass density, $\mathbf{b}$ is the body force, the Cauchy stress σ_{ij} are defined by the generalized Hooke's law

$$\sigma_{ij} = c_{ijkl} \varepsilon_{kl} \text{ in } \widetilde{\Omega} \times [0, T], \tag{2}$$

15

and the components of the strain tensor ε_{ij} obey to the Cauchy relations

$$\varepsilon_{ij} = 1/2\left(u_{i,j} + u_{j,i}\right) \text{ in } \tilde{\Omega}\times\left[0,T\right] \qquad (3)$$

The Neumann and Dirichlet boundary conditions are expressed by

$$\sigma_{ji}n_j = \bar{t}_i \text{ on } \Gamma_t \times\left[0,T\right] \qquad (4)$$

$$u_i = \bar{u}_i \text{ on } \Gamma_u \times\left[0,T\right] \qquad (5)$$

The initial conditions have a form of equalities as follows

$$\mathbf{u}(\mathbf{X},0) = \mathbf{u}_0 \text{ and } \mathbf{v}(\mathbf{X},0) = \mathbf{v}_0 \text{ on } \Omega \qquad (6)$$

The interfacial constitutive law on the discontinuity surfaces should be assigned in terms of the displacements and tractions on each the surfaces as

$$\aleph\left(\mathbf{u}^+,\mathbf{u}^-,\mathbf{t}_c^+,\mathbf{t}_c^-\right) = 0 \text{ on } \Gamma_c \times\left[0,T\right] \qquad (7)$$

Note that we need to distinguish the crack surfaces Γ_c^+ and Γ_c^-, which are smooth and such that $\Gamma_c = \Gamma_c^+ \cup \Gamma_c^-$. Consequently, the current outward unit normals $\mathbf{n}^+$ and $\mathbf{n}^-$, the displacements $\mathbf{u}^+(\mathbf{X},t)$ and $\mathbf{u}^-(\mathbf{X},t)$, and the contact tractions $\mathbf{t}_c^+(\mathbf{X},t)$ and $\mathbf{t}_c^-(\mathbf{X},t)$ are on them. In the case when the surfaces come into contact, there exists the shared common boundary $\Gamma_c = \Gamma_c^+ = \Gamma_c^-$, where the interior continuity conditions on the stresses must be met

$$\sigma_{ji}^+ n_j^+ = \sigma_{ji}^- n_j^- = t_i^c \text{ on } \Gamma_c \times\left[0,T\right] \qquad (8)$$

Therefore, the equations (1-8) represent the strong form of the elastodynamic initial-boundary value problem (IBVP) for a body with a discontinuity. The precise form of the general interface law (7) depends on specific contact conditions accepted for modeling normal and tangential interactions.

2. Contact Modeling. To model contact, we need first to mathematically assert impenetrability along the contact interface. To accomplish this goal, we employ a penetration function g_N to define the normal constraint as follows

$$g_N \equiv \left(\mathbf{x}^+ - \mathbf{x}^-\right)\cdot\mathbf{n}^+ = g_0 + \left(\mathbf{u}^+ - \mathbf{u}^-\right)\cdot\mathbf{n}^+, \qquad (9)$$

where $g_0 = \left(\mathbf{X}^+ - \mathbf{X}^-\right)\cdot\mathbf{n}^+$ is the initial gap. Besides, we need to recall that the point $\mathbf{x}^+$ is closest to the point $\mathbf{x}^-$ in a Euclidean sense, which is being found via the minimal distance problem and the unit normal $\mathbf{n}^+$ to the surface Γ_c^+ is at $\mathbf{x}^+$.

Similarly, to include friction into the problem description we define a tangential slip function $\mathbf{g}_T$ as the vector $\left(\mathbf{x}^+ - \mathbf{x}^-\right)$ projected along unit vectors $\mathbf{a}_\alpha^+$ tangent to the surface Γ_c^+ (Fig. 1b) such that

$$\mathbf{n}^+ = \mathbf{a}_1^+ \times \mathbf{a}_2^+ / \left|\mathbf{a}_1^+ \times \mathbf{a}_2^+\right|$$

It yields the tangent gap vector $\mathbf{g}_T$ as

$$\mathbf{g}_T \equiv \left[\left(\mathbf{x}^+ - \mathbf{x}^-\right) \cdot \mathbf{a}_\alpha^+\right]\mathbf{a}_\alpha^+ = \left[\left(\mathbf{X}^+ - \mathbf{X}^-\right) \cdot \mathbf{a}_\alpha^+ + \left(\mathbf{u}^+ - \mathbf{u}^-\right) \cdot \mathbf{a}_\alpha^+\right]\mathbf{a}_\alpha^+, \quad (10)$$

where the summation convention applies to the pair of the repeated indices.

In the analysis of transient problems, the rate form of the functions defined contact constraints has to be provided. Following by the work [23] we can write

$$\dot{g}_N = \left(\dot{\mathbf{u}}^+ - \dot{\mathbf{u}}^-\right) \cdot \mathbf{n}^+ = \left(\mathbf{v}^+ - \mathbf{v}^-\right) \cdot \mathbf{n}^+ \quad (11)$$

$$\mathsf{L}_\upsilon \mathbf{g}_T = \left(\mathbf{v}^+ - \mathbf{v}^-\right) \cdot \left(\mathbf{a}^\alpha \otimes \mathbf{a}_\alpha\right) \quad (12)$$

Herein the Lie derivative is used to provide a frame invariance of the rate of tangential slip function.

When contact occurs, the traction $\mathbf{t}_c$ on Γ_c can be decomposed into the normal $t_N \mathbf{n}$ and tangential $\mathbf{t}_T$ components such that

$$t_N = -\mathbf{t}_c \cdot \mathbf{n}, \quad (13)$$

$$\mathbf{t}_T = -(\mathbf{I} - \mathbf{n} \otimes \mathbf{n}) \cdot \mathbf{t}_c, \quad (14)$$

where t_N is a scalar that represents the quantity of the contact pressure, and $\mathbf{n}$ is the outward unit normal. It needs to notice that the normal traction (a compressive force) always points inward and the tangent traction (the frictional force) opposes to the relative sliding direction.

With the notations introduced above, we can express the impenetrability conditions in the Kuhn-Tucker form as

$$t_N \geq 0, \ g_N \leq 0 \text{ and } t_N g_N = 0 \quad (15)$$

Generally, contact pairs on the contact interface have two statuses such as sticking or sliding. In the case of sticking there is no tangent sliding between contact pairs, i.e. $\mathbf{g}_T$ vanishes. For tracking the friction phenomenon associated with sliding, the Coulomb friction law is used, which can be expressed in the form of the plasticity framework [23] as follows

$$\Phi(\mathbf{t}_T, t_N) = |\mathbf{t}_T| - \mu t_N \leq 0, \ \mathsf{L}_\upsilon \mathbf{g}_T = \dot{\gamma} \, \mathbf{t}_T / |\mathbf{t}_T|, \ \dot{\gamma} \geq 0, \ \Phi \dot{\gamma} = 0 \quad (16)$$

Thereby, the general interface constitutive law (7) closing the IBVP stated above is now explicitly defined in terms of displacements and tractions over the discontinuity surfaces by constraints in the form of the inequalities (15) and (16).

3. Weak Formulation of the IBVP. To obtain a numerical solution of the local initially boundary value problem formulated in the previous sections a weak or variational form needs to be stated. We first define a specific class of test and trial spaces that are applicable to the finite element method. The displacement trial functions belong to the space of kinematically admissible displacements such that

$$u_i(\mathbf{X}, t) \in U, \ U = \left\{u_i \mid u_i \in C^0(\Omega), u_i = \bar{u}_i \text{ on } \Gamma_u\right\} \quad (17)$$

The space of test functions (or variations of displacements) is defined by

$$\delta u_i(\mathbf{X}) \in U_0, \ U_0 = \left\{\delta u_i \mid \delta u_i \in C^0(\Omega), \delta u_i = 0 \text{ on } \Gamma_u\right\} \quad (18)$$

The weak form of the IBVP can be stated by applying Hamilton's principle

to the body under consideration. The total energy in the body involving intermittent contact with its detached parts will contain two parts wherein the first part comprises the kinetic energy and strain energy, and the second one comes from contribution of the contact tractions at the discontinuity. Then, a typical nonlinear elastodynamic problem defined for the cracked body in the current configuration can be governed by the following variation problem:

Find $u_i(\mathbf{X},t) \in U \times [0,T]$ such that for each $t \in [0,T]$ the stationary conditions of the following variational functional hold

$$\int_\Omega \frac{\partial(\delta u_i)}{\partial x_j} \sigma_{ji} d\Omega - \int_\Omega \delta u_i \rho b_i d\Omega - \int_{\Gamma_t} \delta u_i \bar{t}_i d\Gamma + \int_\Omega \delta u_i \rho \ddot{u}_i d\Omega +$$

$$\int_{\Gamma_c} \left(t_N \delta g_N + \mathbf{t}_T \cdot \delta \mathbf{g}_T \right) d\Gamma = 0, \ \forall \delta u_i(\mathbf{X}) \in U_0 \tag{19}$$

Note that if the Kuhn-Tucker conditions (15) and (16), imposed on the contact boundary Γ_c are satisfied exactly, the contact term in (19) adds nothing to the total energy. However, it is possible only by a true solution, but it is not necessary by the arbitrary test functions. Because the impenetrability dictates $t_N \delta g_N \geq 0$, hence, the corresponding variational formulation (19) takes the form of variational inequality [28]

$$\int_\Omega \frac{\partial(\delta u_i)}{\partial x_j} \sigma_{ji} d\Omega + \int_\Omega \delta u_i \rho \ddot{u}_i d\Omega \geq \int_\Omega \delta u_i \rho b_i d\Omega + \int_{\Gamma_t} \delta u_i \bar{t}_i d\Gamma, \ \forall \delta u_i(\mathbf{X}) \in U_0 \tag{20}$$

Herein, the contact integral provides an additional condition (constraints) to which the stress-strain state of the body has to obey.

The final form of the variational functional (19) will depend on the way with which the constraints will be imposed. Several different approaches are available in literature, for instance, Lagrange multipliers, penalty method, and etc. [23].

Using the mechanical work identity we can recast the variational form such that each of the terms has a physical meaning in the virtual work equation (19),

$$\delta P = \delta P^{int} - \delta P^{ext} + \delta P^{inert} - \delta P^{cont}(t_N, \mathbf{t}_T) = 0, \ \forall \delta u_i(\mathbf{X}) \in U_0 \tag{21}$$

where the symbols sequentially stand the virtual internal work, the virtual external work done by both body forces and prescribed tractions, the virtual work done by body forces in the d'Alembert sense, and the last term is the contact virtual work done by normal and tangential contact forces, respectively.

4. Finite Element Formulation. To solve the variational problem (19) by the FEM, a finite dimensional model of the body should be developed. The domain Ω is subdivided into elements Ω_e so that the union of the elements comprises the total domain, $\Omega = \bigcup_e \Omega_e$. The nodal coordinates in the current configuration are denoted by x_{iI}, $I = 1$ to n_N. We approximate displacement field by the functions from a finite dimensional space $U^h \subset U$, expressed as

$$\mathbf{u}(\mathbf{X},t)= \mathbf{u}_I(t)N_I(\mathbf{X}) \tag{22}$$

where N is the number of discretization nodes in the domain, $\mathbf{u}_I(t)$ are displacements at node I, and $N_I(\mathbf{X})$ is the shape function associated with node I. The velocities and accelerations can be obtained by taking the material time derivatives of the displacements such that

$$\mathbf{v}(\mathbf{X},t)= \dot{\mathbf{u}}_I(t)N_I(\mathbf{X}), \ \ddot{\mathbf{u}}(\mathbf{X},t)= \ddot{\mathbf{u}}_I(t)N_I(\mathbf{X}) \tag{23}$$

The test functions, or variations, are not a function of time, so we approximate the test function within the finite space $U_0^h \subset U_0$ as follows

$$\delta\mathbf{u}(\mathbf{X})= \delta\mathbf{u}_I N_I(\mathbf{X}) \tag{24}$$

where $\delta\mathbf{u}_I$ are the virtual nodal velocities.

To construct the discrete finite element equations, the test functions are substituted into the equation of virtual work (19). Using the arbitrariness of the virtual nodal displacements everywhere except on Γ_u, it then follows that for dynamic contact problem the discretized weak form of the momentum equation expressed in terms of the corresponding nodal forces in accordance with (21) is:

$$\mathbf{M}_{IJ}\ddot{\mathbf{u}}_J = \mathbf{f}_I^{ext} - \mathbf{f}_I^{int} - \mathbf{f}_I^{cont}(t_N,t_T), \ \forall I \notin \Gamma_u \tag{25}$$

Herein the internal nodal forces in the linear case can be defined in terms of the stiffness matrix as

$$f_{iI}^{int} = \int_\Omega N_{I,j}\sigma_{ji}d\Omega = \int_{\Omega_0} N_{I,j}c_{ijkl}N_{J,l}J^0 d\Omega_0 \, u_{kJ} = K_{ikIJ}u_{kJ} \tag{25a}$$

The external nodal forces are calculated by

$$f_{iI}^{ext} = \int_\Omega N_I \rho b_i d\Omega + \int_{\Gamma_t} N_I \bar{t}_i d\Gamma \tag{25b}$$

The inertial nodal forces are computed via the consistent mass matrix as

$$M_{ijIJ}\ddot{u}_{jJ} \equiv f_{iI}^{inert} = \int_\Omega \rho N_I \ddot{u}_i d\Omega = \delta_{ij}\int_{\Omega_0}\rho_0 N_I N_J d\Omega_0 \, \ddot{u}_{jJ} \tag{25c}$$

The explicit form of the vector of contact nodal contact forces depends on a method chosen for implementing contact constraints into the variational equation (19). For instance, in the penalty method for frictionless contact this term can be

$$f_{iI}^{cont} = \int_{\Gamma_c}\varepsilon_N g_N(\mathbf{u})\frac{\partial g_N}{\partial u_{iI}}H(g_N)d\Gamma = \int_{\Gamma_c}\varepsilon_N \Phi_I \Phi_J H(g_N)d\Gamma \, u_{iJ} = K_{IJ}^{cont}u_{iJ}, \tag{25d}$$

where $\Phi_I = \{N_I\mathbf{n}^+ \ if \ I \in \Gamma_c^+ \ or \ N_I\mathbf{n}^- \ if \ I \in \Gamma_c^-\}$, $H(g_N)$ is the Heaviside step function, and ε_N is a penalty parameter. As seen from (25d), the contact forces are mainly defined by the approximation of the surfaces than the shape functions.

Following the usual FEM procedure, the element nodal forces and mass and stiffness matrices are combined from the element level to the global one by an assembly operation. Also the vectors and matrices given in local coordinates are

transformed into the global coordinates. So, the final system of semi-discrete FE equations of motion with Rayleigh damping can be generally expressed by

$$\mathbf{M\ddot{U}} + \mathbf{C\dot{U}} + \mathbf{KU} = \mathbf{F}^{ext} - \mathbf{F}^{cont}\left(\mathbf{U}, t_N, \mathbf{t}_T\right), \qquad (26)$$

where $\mathbf{M}$, $\mathbf{C}$, and $\mathbf{K}$ are the global mass, damping and stiffness matrices, $\mathbf{\ddot{U}}$, $\mathbf{\dot{U}}$, and $\mathbf{U}$ are the vectors of unknown accelerations, velocities and displacements, $\mathbf{F}^{ext}$ and $\mathbf{F}^{cont}$ are the global vectors of external and contact forces.

One may observe that the displacements $\mathbf{U}$ and the contact force $\mathbf{F}^{cont}$ in (26) are both unknowns, as well as contact surfaces, on which the contact constraints must be enforced are not known *a priori*. Therefore, for solving the nonlinear problem (26) an incremental/iterative solution procedure must be used.

The temporal discretization of (26) can be carried out by either implicit or explicit time integration schemes. The explicit procedure requires no the stiffness matrix. The accelerations at the beginning of each time increment (*i*) are directly calculated by

$$\mathbf{\ddot{U}}^{(i)} = \mathbf{\widetilde{M}}^{-1} \cdot \left(\mathbf{F}^{(i)}_{ext} - \mathbf{I}^{(i)}\right), \qquad (27)$$

where $\mathbf{\widetilde{M}}$ is a lumped mass matrix obtained by transform of the consistent mass matrix $\mathbf{M}$, and $\mathbf{I}$ is the common vector of forces updated during the current increment solution step and involving the internal forces, the forces associated with damping and the contact forces. Then, the central difference integration operator is employed to find the nodal velocities and displacements as the following

$$\mathbf{\dot{U}}^{(i+\frac{1}{2})} = \mathbf{\dot{U}}^{(i-\frac{1}{2})} + \frac{\Delta t^{(i+1)} + \Delta t^{(i)}}{2}\mathbf{\ddot{U}}^{(i)} \text{ and } \mathbf{U}^{(i+1)} = \mathbf{U}^{(i)} + \Delta t^{(i+1)}\mathbf{\dot{U}}^{(i+\frac{1}{2})} \quad (28)$$

where the superscripts $(i-1/2)$ and $(i+1/2)$ refer to mid-increment values.

The disadvantage of the explicit procedure is that the time increment used in an analysis must be smaller than the stability limit of the central-difference operator. An approximation to the stability limit is defined by the smallest transit time of a dilatational wave across any of the elements in the FE mesh, [24].

5. Finite Element Model. The approach described above for solving of the elastodynamic problem of the cracked body can be easily adopted within a standard explicit dynamic finite element code. To simulate dynamic responses of sandwich plates involving contact conditions in detached segments of the debonding zone, the ABAQUS/Explicit software [24] is exploited. The finite element model, which is used for the simulation of the dynamic problem, is shown in Fig. 2. The FE model takes the sandwich plate modeling idea of [25]. In the developed model the facesheets are represented as Reissner-Mindlin plates whereas the core is modeled as a three-dimensional continuum. That modeling capability enables to give accurate FE simulations for analyzing a broad range of sandwich plate problems. Especially whenever the core is flexible or localized effects such as a concentrate load applied or debonding phenomenon.

The facesheets are discretized by reduced integrated 8-node continuum shell finite elements, SC8R. These elements discretize an entire three-dimensional body, unlike conventional shell elements, which discretize a reference surface. The SC8R are linear elements and have displacement degrees of freedom only. It should be mentioned that in the case of laminated facesheets, the continuum shell elements were stacked to provide a more refined through-the-thickness response of transverse shear stresses and forces. Because, the continuum shell elements can be connected directly to first-order continuum solids without any kinematic transition, 8-node isoparametric linear solid 'brick' elements with incompatible
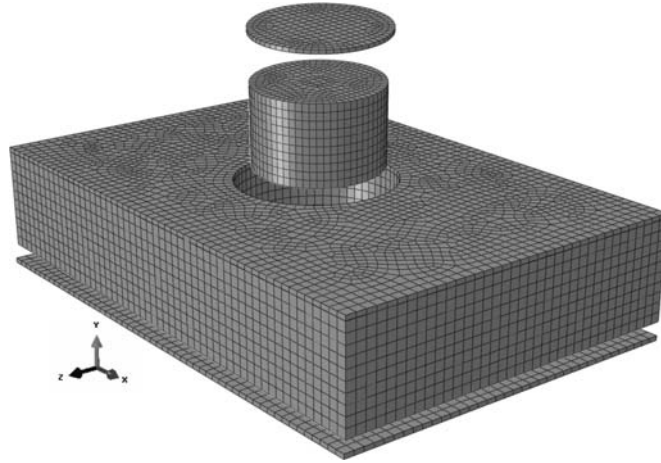

Fig.2. 3-D FE model of a sandwich plate with a penny-shaped debonding zone.

mode C3D8I were chosen for core modeling. In addition to the standard displacement degrees of freedom (three translations in each a node), incompatible deformation mode is added internally to the elements in order to eliminate the parasitic shear stresses that cause the response of the regular first-order displacement elements to be too stiff in bending. For detailed information concerning element technology we are referred to [24]. The shell elements were positioned on the upper and lower core sides and were directly connected to the core through their share nodes. The debonding was introduced by an actual small gap in a certain zone between the facesheet and the core. The mesh density of the sandwich plate was higher in the part, where the debonding zone was defined.

The contactable parts of the facesheet and the core at the damaged interface of the vibrating sandwich plate were simulated by using the surface-to-surface discretization method. The relative motion of the interacting surfaces was described with small displacements kinematics. The contact behavior of the surfaces coming into contact in the normal direction was governed by the 'hard contact' model, that is the interacting surfaces transmit no contact pressure unless the nodes of the slave surface contact the master surface and no penetration is allowed at each constraint location. The frictionless conditions were accepted between the surfaces interacted in the tangential direction. In the dynamic analysis the normal contact constraints were implemented using the penalty algorithm.

6. Numerical Results. The FE simulations are employed to obtain a deep insight of the debonded sandwich plate dynamics. The free vibration, dynamic transient and dynamic steady-state analyses of sandwich plates containing the debonding zone were carried out within the ABAQUS code. One configuration of a sandwich plate is throughout used in this study. A simply supported rectangular sandwich plate of 180 mm by 270 mm consisting of a 50 mm-thick WF51 foam core and 2.4 mm-thick GFRP face sheets and damaged by a penny-shaped debonding zone of a 40 mm radius at its center is being analyzed. Mechanical properties of the constituent materials are given in Table 1.

The transient response of the debonded sandwich plate was first examined. The plate was excited by an impulse force at the central point of the bottom face sheet. The duration of the applied impulse force was much shorter than the analysis time such that

$$F(t) = \begin{cases} F_0, 0 \leq t \leq t_* \\ 0, \quad t \geq t_* \end{cases},$$

with $t_* = 1 ms$ and $F_0 = 1 kN$.

Table 1. Material properties of the foam-cored sandwich plate.

Components	Elastic constants
Foam core	$E_C = 85\ MPa$, $G_C = 30\ MPa$, $\rho_C = 52\ kgm^{-3}$
GFRP facesheet	$E_{xx} = E_{zz} = 19.3\ GPa$, $\quad E_{yy} = 3.48\ GPa$, $\quad G_{xy} = G_{yz} =$ 1.65 GPa, $G_{zx} = 7.7\ GPa$, $\rho = 1650\ kgm^{-3}$

Time histories corresponding to a transverse displacement and a longitudinal strain, calculated at the central point of the upper facesheet, for the same plates with and without debonding are compared in Fig.4. Moreover, in the case of the existence of debonding two FE models with and without contact conditions at the debonding region were applied. As one can see that the presence of the debonding zone significantly affects on the impulse response of the plate, and the period of the free decay vibration for the debonded plate is longer than for the intact one. It can be explained by the stiffness reduction due to the presence of debonding. The comparative results between plates, accounting for and not accounting for contact allow concluding that the neglect of contact significantly overestimates the time history amplitudes and, thereby, leads to misleading results.

To provide a deeper insight into dynamics of sandwich plates with debonding, their steady-state dynamic responses are further examined. The same sandwich plate as in the previous analysis is subjected to a concentrated transverse sinusoidal force at the central point of the lower skin with the amplitude of 1 *kN*. The frequency of the exciting force is 1000 *Hz* that is close to the fundamental frequency of the sandwich plate. The calculations showed that the interaction at the detached surfaces in the steady-state motion plays an important role. Namely, one can see from Fig. 5, a pure sinusoidal waveform

corresponds to the steady-state histories of displacement and velocity of the intact plate, whereas the same signals for the debonded plate are either modulated as for the displacement or have absolutely lost their periodicity as for the velocity. Moreover, the magnitude of the velocity signal in the plate with debonding is remarkably greater. These results clearly demonstrate the non-linearity of the debonded plate's dynamics. Thereby, the typical assumption that if excitations are harmonic, then the response is also harmonic, commonly used in linear system is no longer valid for the nonlinear system. Instead, the steady-state response of such systems described easily by modal approaches should be studied based on the general dynamic analysis with a periodic function. Fig. 6 presents the deformed shapes of the debonded sandwich plate corresponding to two main statuses such as open debonding and closed one.
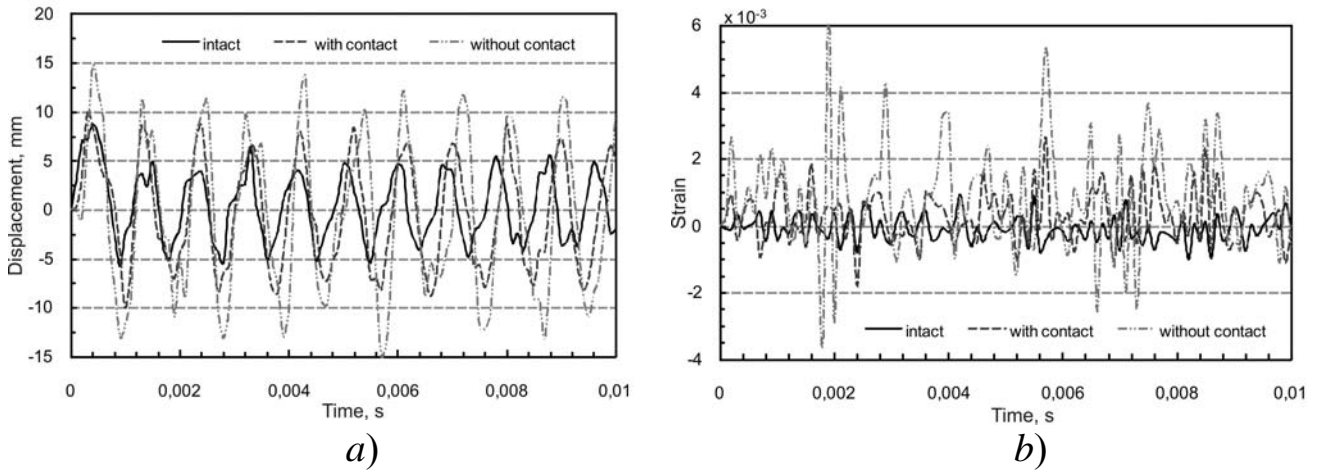

a) *b)*

Fig.4. Transient time histories at the central point: displacement (a) and strain (b).
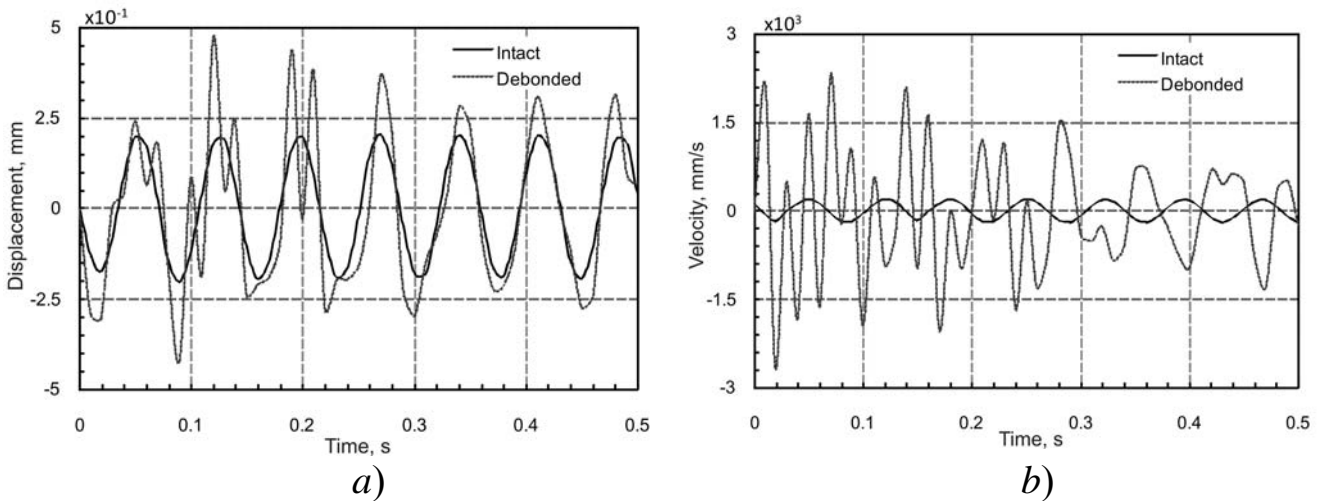

a) *b)*

Fig.5. Steady-state time history responses at the central point: displacement (a) and velocity (b).

7. Conclusions. The FE formulation is applied to study dynamics of the debonded foam-cored sandwich plate subjected to both impulse and harmonic loads. The numerical results show that in order to model accurately dynamics of debonded sandwich plates, the contact phenomenon has to be mandatory be

taking into account within the debonding region. The results also indicate that an impulse response and a steady-state response of debonded sandwich plates are remarkable affected by the presence of debonding. For the latter the steady-state dynamic analyses based on modal approaches are no longer valid.
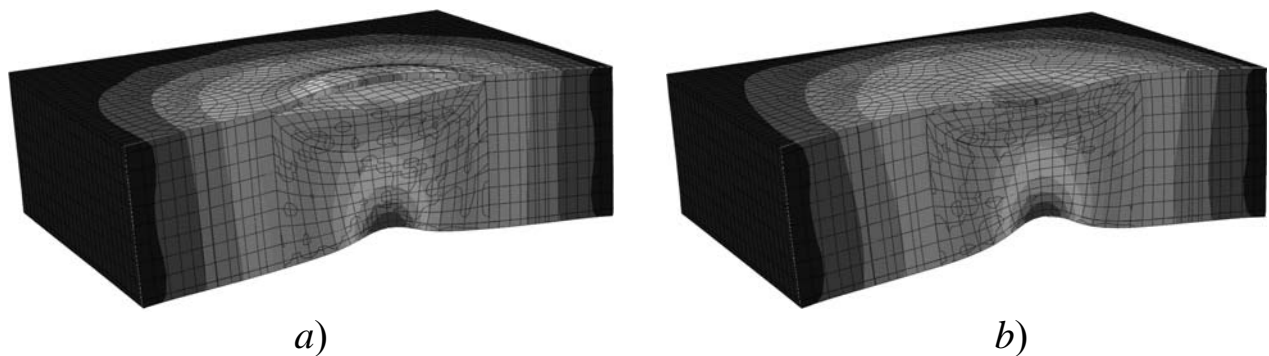

a)   *b)*

Fig.6. Deformed shapes of the debonded sandwich plate at a time moment corresponding to open debonding (a) and closed debonding (b).

REFERENCES

1. Ramkumar R.L., Kulkarni S.V., Pipes R.B. Free vibration frequencies of a delaminated beam. In: 34th Annual Technical Conference, Reinforced Plastic/Composite Institute, The Society of the Plastics Industry, 1979, p. 1–5.
2. Wang J.T.S., Lin Y.Y., Gibby J.A. Vibration of split beams. Journal of Sound and Vibration, 84, 1982, p. 491–520.
3. Majumdar P.M., Suryanarayn S. Flexural vibration of beams with delaminations. Journal of Sound and Vibration, 125, 1988, p. 441–461.
4. Luo H., Hanagud S. Dynamics of delaminated beams. International Journal of Solids and Structures, 37, p. 1501–1519.
5. Wang J., Tong L. A study of the vibration of delaminated beams using a nonlinear anti-interpenetration constraint model. Composite Structure, 57, 2002, p. 483–488.
6. Zak A., Krawczuk M., Ostachowicz W. Numerical and experimental investigation of free vibration of multilayer delaminated composite beams and plates. Computational Mechanics, 26, 2000, p. 309–315.
7. Bachene M., Tiberkak R., Rechak S. Vibration analysis of cracked plates using the extended finite element method. Archive of Applied Mechanics, 79(3), 2009, p. 249-262.
8. Tenek L.H., Hennekke E.G., Gunzburger M.D. Vibration of delaminated composite plates and some applications to non-destructive testing. Composite

Structures, 23, 1993, p. 253–262.

9. Burlayenko V.N., Sadowski T. Influence of skin/core debonding on free vibration behavior of foam and honeycomb cored sandwich plates. International Journal of Non-Linear Mechanics, 45(10), 2010, p. 959-968.

10. Della C.N., Shu D. Vibration of delaminated composite laminates: a review. Applied Mechanics Reviews, 60, 2007, p. 1–20.

11. Montalvão D., Maia N.M.M., Ribeiro A.M.R. A review of vibration-based structural health monitoring with special emphasis on composite materials. Shock and Vibration Digest, 38(4), 2006, p. 295-234.

12. Matveev V. V., Bovsunovskii A. P. Some aspects of vibration of an elastic body with a "breathing" discontinuity of material. Strength of Materials, 32(5), 2000, p. 434-445.

13. Chondros T.G., Dimarogonas A.D., Yao J. Vibration of a beam with a breathing crack. Journal of Sound and Vibration, 239(1), 2001, p. 57–67.

14. Vielsack P. A vibro-impacting model for the detection of delamination. Journal of Sound and Vibration, 253(2), 2002, p. 347–358.

15. Zozulya V.V., Conzalez-Chi P.I. Dynamic fracture mechanics with contact ionteraction at the crack edges. Engineering Analysis with Boundary Elements, 24, 2000, p. 643-659.

16. Ju F., Lee H.P., Lee K.H. Dynamic responses of delaminated composite beams with intermittent contact in delaminated segments. Composites Engineering, 4(12), p. 1211-24.

17. Ju F., Lestari W., Hanagud S. Nonlinear vibrations of a delaminated beam. Journal of Sound and Control, 7, 2001, p. 803-831.

18. Fu Y., Zhang Y. Nonlinear vibration of beam-plates with a delamination. Acta Mechanica Solida Sinica, 13(4), 2000, p. 353-362.

19. Kwon Y.W., Lannamann D.L Dynamic numerical modeling and simulation of interfacial cracks in sandwich structures for damage detection. Journal of Sandwich Structures and Materials, 4, 2002, p. 175-199.

20. Oh J., Cho M., Kim J.-S. Dynamic analysis of composite plate with multiple delaminations based on higher-order zigzag theory. International Journal of Solids and Structures, 42, 2005, p. 6122-40.

21. Schwarts-Givli H., Rabinovitch O., Frostig Y. High-order nonlinear contact effects in the dynamic behavior of delaminated sandwich panels with a flexible core. International Journal of Solids and Structures, 44, 2007, p. 77–99.

22. Burlayenko V.N., Sadowski T. A numerical study of the dynamic response of sandwich plates initially damaged by low velocity impact. Computational Material Science, 52(1), 2012, p. 212-216.

23. Laursen T.A. Computational contact and impact mechanics: fundamentals of modeling interfacial phenomena in nonlinear finite element analysis. – Berlin, Springer-Verlag, 2002. – 454 p.

24. ABAQUS User Manual Version 6.9EF-1 (2009) Dassault Systèmes Simulia Corp. Providence, RI, USA.

25. Frostig Y., Thomsen O.T. High-order free vibration of sandwich panels with a flexible core. International Journal of Solids and Structures, 41, 2004, p. 1697–1724.

Burlayenko V. N., Sadowski T., Nazarenko S.A. Numerical modeling of dynamics of sandwich plates with partially damaged facesheet-to-core interface

UDC 74K20

A finite element (FE) model has been developed for analysis of the dynamic response of sandwich plates with partially damaged facesheet-to-core interface. The effect of intermittent dynamic contact between the fragments detached at the damaged interface is taken into account in the vibrating sandwich plate. The general mathematical statement of such non-linear elastodynamic problem for a cracked body is first formulated. Numerical results for the transient and steady-state dynamic responses of a foam-cored sandwich plate damaged by debonding are obtained by using the ABAQUS code. The influence of the strongly non-linear local contact behavior on dynamics of the sandwich plate is examined.